

# Combination of palladium nanoparticles and tubastatin-A potentiates apoptosis in human breast cancer cells: a novel therapeutic approach for cancer

Yu-Guo Yuan<sup>1</sup>  
Qiu-Ling Peng<sup>2</sup>  
Sangiliyandi Gurunathan<sup>3</sup>

<sup>1</sup>College of Veterinary Medicine/ Animal Science and Technology/ Jiangsu Co-Innovation Center for Prevention and Control of Important Animal Infectious Diseases and Zoonosis, Yangzhou University, Yangzhou, <sup>2</sup>College of Chemistry and Bioengineering, Yichun University, Yichun, People's Republic of China; <sup>3</sup>Department of Stem cell and Regenerative Biotechnology, Konkuk University, Seoul, Republic of Korea

**Background:** Breast cancer is the most common malignant disease that occurs in women. Histone deacetylase (HDAC) inhibition has recently emerged as an effective and attractive target for the treatment of cancer. The aim of this study was to investigate the efficacy of a combined treatment of tubastatin A (TUB-A) and palladium nanoparticles (PdNPs) against MDA-MB-231 human breast cancer cells using two different cytotoxic agents that work by two different mechanisms, thereby decreasing the probability of chemoresistance in cancer cells and increasing the efficacy of toxicity, to provide efficient therapy for advanced stage of cancer without any undesired side effects.

**Methods:** PdNPs were synthesized using a novel biomolecule called R-phycoerythrin and characterized using various analytical techniques. The combinatorial effect of TUB-A and PdNPs was assessed by various cellular and biochemical assays and also by gene expression analysis.

**Results:** The biologically synthesized PdNPs had an average size of 25 nm and were spherical in shape. Treatment of MDA-MB-231 human breast cancer cells with TUB-A or PdNPs showed a dose-dependent effect on cell viability. The combination of 4  $\mu$ M TUB-A and 4  $\mu$ M PdNPs had a significant inhibitory effect on cell viability compared with either TUB-A or PdNPs alone. The combinatorial treatment also had a more pronounced effect on the inhibition of HDAC activity and enhanced apoptosis by regulating various cellular and biochemical changes.

**Conclusion:** Our results suggest that there was a strong synergistic interaction between TUB-A and PdNPs in increasing apoptosis in human breast cancer cells. These data provide an important preclinical basis for future clinical trials on this drug combination. This combinatorial treatment increased therapeutic potentials, thereby demonstrating a relevant targeted therapy for breast cancer. Furthermore, we have provided the first evidence for the combinatorial effect and mechanism of toxicity of TUB-A and PdNPs in human breast cancer cells. The novelties of the study were identification of a combination therapy that consists of suitable therapeutic molecules that kill cancer cells and also exploration of two different possible mechanisms involved to reduce chemoresistance in cancer cells.

**Keywords:** tubastatin A, palladium nanoparticles, cell viability, oxidative stress, mitochondrial membrane potential, caspases, apoptosis

Correspondence: Yu-Guo Yuan  
College of Veterinary Medicine,  
Yangzhou University, 48 Wenhui  
Road, Yangzhou, Jiangsu 225009,  
People's Republic of China  
Tel +86 514 8797 9228  
Fax +86 514 8797 2218  
Email yyg9776430@163.com

Sangiliyandi Gurunathan  
Department of Stem cell Biology  
and Regenerative Biology, Konkuk  
University, 120 Gwangjin-gu,  
Seoul 143-701, Korea  
Tel +82 2 450 0581  
Email gsangiliyandi@yahoo.com

## Introduction

Cancer is a group of diseases that cause cells in the body to change and grow out of control, which results from defects in genes, such as mutations, deletions, and

chromosomal abnormalities.<sup>1-3</sup> Breast cancer is the most common malignant disease that occurs in women worldwide, with 522,000 breast cancer-related deaths in 2012 and 1.67 million new cases being diagnosed every year.<sup>4</sup> Breast cancer is typically detected either during a screening examination, before symptoms have developed, or after a woman notices a lump. According to the American Cancer Society, 231,840 new cases of invasive breast cancer as well as an estimated 60,290 additional cases of in situ breast cancer were diagnosed among women in 2015, and 40,290 women are expected to die from the disease.<sup>5</sup> Chemotherapy seems to be an effective treatment to eliminate cancer cells. Among many cancer chemotherapeutic strategies, platinum-based drugs, nitrogen mustards, and drugs like temozolomide are the most frequently used.<sup>6</sup> However, because DNA alkylating agents produce toxic side effects, the platinum-based drugs, such as cisplatin, are used instead for the treatment of many types of cancers.

For several years, targeted cancer therapy has been considered to be among the most promising developments for obtaining high therapeutic effects with negligible toxicity.<sup>7</sup> One of the vital strategies to increase the efficacy of conventional chemotherapeutic and molecular-targeted drugs or nanotherapy is by combining two low doses of potential therapeutic agents, such as histone deacetylase (HDAC) inhibitors (HDACIs) and nanoparticles (NPs).<sup>7,8</sup> Recent preclinical studies have reported HDACIs to be potential therapeutic agents for killing cancer cells, owing to their broad anticancer potency and low toxicity. Combinatorial therapy plays a major role in minimizing drug resistance, undesired side effects, and chemoresistance, which are critical problems in cancer therapy.<sup>9</sup> HDACIs have the capacity to kill cancer cells through various mechanistic approaches, such as by controlling the transcription and regulation of genes involved in the cell cycle, cell proliferation, cell survival, and DNA repair, and by inducing the expression of pro-apoptotic proteins. NPs, on the other hand, kill cancer cells by elevating oxidative stress, collapsing the mitochondrial membrane potential (MMP;  $\Delta\Psi_m$ ), and increasing pro-apoptotic gene expression and DNA fragmentation.<sup>8</sup> HDACs regulate the acetylation of a variety of histone and non-histone proteins, thereby controlling the transcription and regulation of genes involved in cell cycle control, proliferation, survival, DNA repair, and differentiation.<sup>10</sup> Preclinical evidence has shown that adding HDAC as a target to a diverse range of standard chemotherapeutic agents leads to the synergistic induction of cancer cell death, demonstrating the utility of a multitargeted approach involving HDAC modulation in the treatment

of cancer. Therefore, targeting HDAC activity through the use of HDACIs has become a novel and alternative therapeutic strategy for cancer.<sup>11</sup> Histone acetylation and deacetylation are critical in biological processes as they regulate the modification of chromatin structures and are hence important for gene regulation.<sup>12</sup>

HDAC6 is especially well suited for specific inhibition, owing to its unique domain structure and mode of action, and has been suggested to provide an exceptionally suitable target for cancer therapy.<sup>13</sup> Rosik et al<sup>13</sup> evaluated the efficacy of three different HDAC6-specific inhibitors (viz., tubacin, tubastatin A [TUB-A], and ST-80) in urothelial carcinoma cells. HDACIs are able to reduce cell survival in human breast cancer cells by remodeling human epidermal growth factor receptor 2 (HER2) promoters and HER2 expression,<sup>14</sup> and they can induce mitochondrial reactive oxygen species (ROS) production.<sup>15</sup> These inhibitors have, therefore, been found to be effective as anticancer agents, at least for some types of cancers like cutaneous T-cell lymphoma, by promoting the expression of tumor suppressor genes and inducing cell differentiation, growth arrest, and/or apoptosis.<sup>16-18</sup>

To overcome off-target effects, onset of drug resistance, and cancer recurrences from chemotherapeutic agents, as well as poor drug solubility and low bioavailability, the use of NPs as cytotoxic or delivery agents seems to be an alternative and viable technology; NPs are thus emerging as a class of therapeutics for cancer. Clinical studies suggest that NPs show enhanced efficacy and minimal side effects as a result of their more targeted localization in tumors and active cellular uptake.<sup>19</sup> Recently, several inorganic NPs, including silver, palladium (Pd), and gold, have been used as anticancer agents in various types of cancer cells.<sup>20-22</sup> Generally, studies that applied palladium nanoparticles (PdNPs) were mainly interested in hydrogen storage and sensing,<sup>23</sup> catalysis,<sup>24</sup> hydrogenation,<sup>25</sup> oxidation,<sup>26</sup> carbon-carbon bond formation,<sup>27</sup> and fuel cells,<sup>28</sup> but not cancer. Studies on the anticancer effects of PdNPs are very limited, and so far, there has been no report about the combinatorial effect of TUB-A and PdNPs on human breast cancer cells. Conventional adjuvant therapies such as radiotherapy and chemotherapy have had little beneficial effect in the advanced stage of cancer, with undesired side effects. Generally, monotherapy has been only partially effective on particular disease, whereas combination therapy could enhance tolerability because two compounds may be employed below their individual dose thresholds to minimize side effects. Therefore, the goal of this study was to use combination therapy that consists of two different cytotoxic agents with optimal doses that work

by different mechanisms, which could thereby decrease the probability of chemoresistance. Based on this concept, this study was designed to address three main objectives: 1) the synthesis and characterization of PdNPs using a novel biomolecule, R-phycoerythrin (RPE); 2) evaluation of the efficacy of combined TUB-A and PdNPs treatment in human breast cancer cells; and 3) investigation of the cytotoxic mechanism of these two different agents.

## Materials and methods

### Materials

Penicillin–streptomycin solution, trypsin–EDTA solution, RPMI-1640 medium, and 1% antibiotic–antimycotic solution were obtained from Life Technologies/Gibco (Grand Island, NY, USA). PdCl<sub>2</sub> for the preparation of PdNPs, RPE, TUB-A, fetal bovine serum (FBS), and in vitro toxicology assay kit were purchased from Sigma-Aldrich (St Louis, MO, USA). All other chemicals were also purchased from Sigma-Aldrich unless otherwise stated.

### Synthesis and characterization of PdNPs

PdNPs were prepared using RPE according to a previously described method with required modification.<sup>21</sup> In a typical experiment, the reaction mixture was prepared by suspending 10 mL of RPE (4 μM) in 10 mL of sterile distilled water and this was mixed well for 5 min and then added to 90 mL of 1 mM PdCl<sub>2</sub> solution in a 250 mL round bottom flask, which was mounted with a cooling condenser and a magnetic stir bar. The mixture was stirred for 2 h at 60°C with constant stirring. A reduction reaction occurred rapidly which was evidenced by a change in the color of the solution from light yellow to bright brown. After 2 h, the mixture was allowed to cool down followed by centrifugation (10,000 rpm). On washing the mixture three times with distilled water, a black powder was obtained, which was dried overnight in an oven at 80°C.

Characterization of PdNPs was performed according to a previously described method.<sup>21</sup> Spectra of the synthesized PdNPs were recorded using a ultraviolet (UV)-visible spectrophotometer from 300 nm to 600 nm. X-ray diffraction (XRD) analyses were performed using a Bruker D8 Discover X-ray diffractometer (Bruker AXS GmbH, Karlsruhe, Germany). The X-ray source was 3 kW with a Cu target, and high-resolution XRD patterns were measured using a scintillation counter ( $\lambda=1.5406 \text{ \AA}$ ). The XRD was run at 40 kV and 40 mA, and samples were recorded at 2 $\theta$  values between 10° and 80°. The dried PdNPs powder was diluted with potassium bromide, Fourier transform infrared spectroscopy (FTIR; Perkin Elmer Inc., Waltham, MA,

USA) was performed, and the spectra were recorded within a range of 500–4,000 cm<sup>-1</sup>. The particle size of dispersions was measured by a Zetasizer Nano ZS90 (Malvern Instruments, Malvern, UK). Transmission electron microscopy (TEM) was performed with a TEM Hitachi H-7500 to determine the size and morphology of PdNPs with images obtained at an accelerating voltage of 300 kV.

### Cell culture

MDA-MB-231 human breast cancer cells were obtained from Sigma-Aldrich and grown adherently and maintained in RPMI-1640 medium containing 10% FBS and 1% antibiotic solution (penicillin plus streptomycin) at 37°C under 5% CO<sub>2</sub>. All experiments were performed in six-well plates, unless otherwise stated. Cells were seeded into the plates at a density of 1×10<sup>6</sup> cells/well and incubated for 24 h prior to the experiments.

### Cell viability assay

The WST-8 assay was performed as described previously.<sup>21</sup> Typically, 2×10<sup>5</sup> cells/well were seeded into a 96-well plate and cultured in RPMI-1640 standard medium supplemented with 10% FBS at 37°C under 5% CO<sub>2</sub>. After 24 h, the cells were washed twice with 100 μL of serum-free RPMI-1640 and then incubated with 100 μL of medium containing TUB-A (2–20 μM) or PdNPs (2–20 μM) for 24 h. Cells not exposed to TUB-A or PdNPs served as controls. After 24 h of drug exposure, the cells were washed twice with serum-free RPMI-1640. Each well was then replenished with 100 μL of serum-free RPMI-1640, following which 15 μL of WST-8 solution was added. After 1 h of incubation at 37°C under 5% CO<sub>2</sub>, 80 μL of the mixture was transferred to another 96-well plate and the absorbance was measured at 450 nm using a microplate reader.

### Cell morphology

MDA-MB-231 human breast cancer cells were plated in six-well plates (2×10<sup>5</sup> cells/well) and incubated with TUB-A (20 μM) or PdNPs (4 μM) or a combination of TUB-A (4 μM) and PdNPs (4 μM) for 24 h. Cells cultured in medium without the addition of TUB-A or PdNPs were used as the control. At 24 h post-treatment, the morphology of the cells was examined under an Olympus IX71 microscope (Olympus Corporation, Tokyo, Japan), using appropriate filter sets.

### HDAC activity

HDAC activity was analyzed according to a previously described method.<sup>29</sup> MDA-MB-231 human breast cancer

cells were treated with TUB-A (4  $\mu\text{M}$ ) or PdNPs (4  $\mu\text{M}$ ) or a combination of TUB-A (4  $\mu\text{M}$ ) and PdNPs (4  $\mu\text{M}$ ) for 24 h. The cells were then washed with phosphate-buffered saline (PBS) and resuspended in five volumes of a lysis buffer (R&D Systems, Inc., Minneapolis, MN, USA). Next, the cells were harvested, and whole-cell protein was extracted using RIPA lysis buffer. Protein concentrations were determined with a bicinchoninic acid kit. Supernatant samples containing 20  $\mu\text{g}$  of total protein were used for the determination of HDAC activity, which was measured using an HDAC Activity Assay Kit (Sigma-Aldrich) according to the manufacturer's instructions. The samples were added to each well of a 96-well microtiter plate together with HDAC substrate provided in the assay kit and incubated at 37°C for 1 h.

### Cytotoxicity assay

The cell membrane integrity of human breast cancer cells was evaluated as described previously,<sup>20</sup> by determining the release of lactate dehydrogenase (LDH) from the cells, using an in vitro toxicology assay kit (TOX7; Sigma-Aldrich) according to the manufacturer's instructions. In brief, the cells were exposed to TUB-A (4  $\mu\text{M}$ ) or PdNPs (4  $\mu\text{M}$ ) or a combination of TUB-A (4  $\mu\text{M}$ ) and PdNPs (4  $\mu\text{M}$ ) for 24 h, and then the LDH content was measured.

The amount of ROS in the cells was also estimated according to a previously described method.<sup>20</sup> The cancer cells were seeded into 24-well plates at a density of  $5 \times 10^4$  cells/well and cultured for 24 h. After washing twice with PBS, fresh medium containing TUB-A (4  $\mu\text{M}$ ) or PdNPs (4  $\mu\text{M}$ ) or a combination of TUB-A (4  $\mu\text{M}$ ) and PdNPs (4  $\mu\text{M}$ ) was added and the plates were incubated for 24 h. The cells were then supplemented with 20  $\mu\text{M}$  2',7'-dichlorofluorescein diacetate ( $\text{H}_2\text{DCFDA}$ ), and incubated further for 30 min at 37°C. After rinsing the cells with PBS, 2 mL of PBS was added to each well, and the fluorescence intensity was determined using a spectrofluorometer (Gemini EM, Molecular Devices, Sunnyvale, CA, USA) with excitation at 485 nm and emission at 530 nm.

### Measurement of oxidative stress markers

Assays for the oxidative stress markers malondialdehyde (MDA), glutathione (GSH), superoxide dismutase (SOD), and catalase (CAT) were performed using reagent kits (Sigma-Aldrich) according to the manufacturer's instructions. In brief, the cancer cells were cultured in 75  $\text{cm}^2$  culture flasks and exposed to TUB-A (4  $\mu\text{M}$ ) or PdNPs (4  $\mu\text{M}$ ) or a combination of TUB-A (4  $\mu\text{M}$ ) and PdNPs (4  $\mu\text{M}$ ) for 24 h. Following this, the cells were harvested in chilled PBS by scraping and then washed twice with  $1 \times$  PBS at 4°C for 6 min

at 1,500 rpm. The cell pellet was sonicated at 15 W for 10 s (3 cycles) to obtain a cell lysate, and the resultant supernatant was stored at  $-70^\circ\text{C}$  until analysis.

### Mitochondrial membrane potential

The cells were cultured in 75  $\text{cm}^2$  culture flasks and exposed to TUB-A (4  $\mu\text{M}$ ) or PdNPs (4  $\mu\text{M}$ ) or a combination of TUB-A (4  $\mu\text{M}$ ) and PdNPs (4  $\mu\text{M}$ ) for 24 h. Then,  $\Delta\Psi_m$  was measured as described previously,<sup>30</sup> using cationic fluorescent indicator JC-1 (Molecular Probes, Eugene, OR, USA). JC-1 is a lipophilic cation that, in a reaction driven by  $\Delta\Psi_m$  in normal polarized mitochondria, assembles into a red fluorescence-emitting dimer to form JC-1 aggregates. Cells were incubated with 10  $\mu\text{M}$  JC-1 at 37°C for 15 min and then washed with and resuspended in PBS; after that, the fluorescence intensity was measured. The  $\Delta\Psi_m$  value was expressed as the ratio of the fluorescence intensity of the JC-1 aggregates to that of the monomers.

### Measurement of caspase-3 activity and terminal deoxynucleotidyl transferase dUTP nick end labeling (TUNEL) assay

Measurement of caspase-3 and the TUNEL assay were performed according to previously described methods.<sup>31</sup> The cancer cells were treated with TUB-A (4  $\mu\text{M}$ ) or PdNPs (4  $\mu\text{M}$ ) or a combination of TUB-A (4  $\mu\text{M}$ ) and PdNPs (4  $\mu\text{M}$ ) for 24 h, with the addition of caspase-3 inhibitor for 24 h. The activity of caspase-3 in the cells was measured using a commercial kit (Sigma-Aldrich) according to the manufacturer's instructions.

For the TUNEL assay, cells were treated with TUB-A (4  $\mu\text{M}$ ) or PdNPs (4  $\mu\text{M}$ ) or a combination of TUB-A (4  $\mu\text{M}$ ) and PdNPs (4  $\mu\text{M}$ ) for 24 h, and apoptosis was determined using a DNA Fragmentation Imaging Kit (Roche Diagnostics, Basel, Switzerland) according to the manufacturer's instructions. After the incubation period, the culture medium was aspirated and the cell layers were trypsinized. The trypsinized cells were reattached on 0.01% polylysine-coated slides, fixed with 4% methanol-free formaldehyde solution, and stained according to the manufacturer's instructions.

### mRNA extraction and amplification

Total RNA was extracted from cells treated with TUB-A (4  $\mu\text{M}$ ) or PdNPs (4  $\mu\text{M}$ ) or a combination of TUB-A (4  $\mu\text{M}$ ) and PdNPs (4  $\mu\text{M}$ ) for 24 h, using Arcturus PicoPure RNA isolation kit (eBioscience, San Diego, CA, USA), and samples were prepared according to the manufacturer's instructions. Quantitative reverse transcription polymerase chain reaction (qRT-PCR) was conducted using a Vill7 system (Applied

**Table 1** Primers used for quantitative real time reverse transcription polymerase chain reaction for the analysis of apoptotic, and anti-apoptotic, gene expression

Serial number	Gene	Direction	Primers (5'-3')
1	Bax	F	GAG AGG TCT TTT TCC GAG TGG
		R	GGA GGA AGT CCA ATG TCC AG
2	p53	F	AGG AAA TTT GCG TGT GGA GTA T
		R	TCC GTC CCA GTA GAT TAC CAC T
3	Bak	F	CTC AGA GTT CCA GAC CAT GTT G
		R	CAT GCT GGT AGA CGT GTA GGG
4	CAS-3	F	CAT ACT CCA CAG CAC CTG GTT A
		R	ACT CAA ATT CTG TTG CCA CCT T
5	CAS-9	F	ACT TTC CCA GGT TTT GTT TCC T
		R	GAA ATT AAA GCA ACC AGG CAT C
6	Bcl-2	F	CTG AGT ACC TGA ACC GGC A
		R	GAG AAA TCA AAC AGA GGC CG

**Abbreviations:** F, forward; R, reverse.

Biosystems, Foster City, CA, USA) and SYBR Green as the double-stranded DNA-specific fluorescent dye (Applied Biosystems). Target gene expression levels were normalized to that of *GAPDH* expression, which was unaffected by treatment. The RT-PCR primer sets used are shown in Table 1. Real-time RT-PCR was performed independently, in triplicates, for each of the different samples. The data are presented as the mean values of gene expression measured in treated samples versus the control.

## Statistical analyses

All assays were conducted in triplicates, and each experiment was repeated at least three times. The results represent the mean of at least three independent experiments (mean  $\pm$  SD). Student's *t*-test or one-way analysis of variance followed by Tukey's test was applied for multiple comparisons, using Graph-Pad Prism software (GraphPad Software, San Diego, CA, USA). The differences were considered significant at  $P < 0.05$ .

## Results and discussion

### Synthesis and characterization of PdNPs

The synthesis of PdNPs was performed at 60°C using an aqueous solution of PdCl<sub>2</sub>, with RPE as a reducing and stabilizing agent. The color of the aqueous PdCl<sub>2</sub> solution changed gradually from light yellow to dark brown following the addition of RPE, indicating the formation of PdNPs.<sup>21</sup> The UV-visible (Vis) spectrum of the aqueous PdCl<sub>2</sub> solution showed a sharp and significant peak at 420 nm, and a broad continuous absorption was observed after the reduction reaction, which indicated the complete reduction of Pd(II) ions to PdNPs (Figure 1A). Previous reports have suggested that phycobiliproteins can be used to synthesize NPs.

Synthesis of AgNPs was performed using *Spirulina platensis*, a blue-green microalgae (cyanobacteria) known to have phycobiliproteins.<sup>32,33</sup> Bekasova et al<sup>34</sup> demonstrated the synthesis of AgNPs using RPE extracted from the red alga *Callithamnion rubosum*. Our data are consistent with these publications suggesting that phycobiliproteins are able to reduce PdCl<sub>2</sub>. Taken together, these experiments suggest that protein-based pigments from cyanobacteria are able to mediate the formation of NPs in a non-toxic manner, because of the presence of amino acids, vitamins, and carbohydrates. Therefore, we explored the possibility of synthesis of PdNPs using RPE.

X-ray diffraction results showed four different peaks, which corresponded to reflections from the (111), (200), (220), and (311) planes of the face-centered cubic lattice, respectively (Figure 1B).<sup>21,35</sup> As shown in Figure 1C, the major absorbance bands were observed at 3,314 and 1,635 cm<sup>-1</sup>, corresponding to the hydrogen-bonded hydroxyl (OH) and amide I groups, respectively. The bands found at 1,635 cm<sup>-1</sup> could be due to the characteristic asymmetrical stretch of the carboxylate and carbonyl groups and the characteristic peaks of aromatic C–C stretching.<sup>8</sup> The size distribution analysis showed the average size of the PdNPs to be 25 nm (Figure 1D). The mean particle size was found to be 25 nm. The polydispersity index and zeta potential (mV) of the PdNPs were 0.113 and –0.35 (mV), respectively. To determine size consistency, TEM images of the PdNPs were taken, which showed that all of the particles were spherical in shape, dispersed within a range of 10–60 nm, and had an average particle size of 25 nm (Figure 1E and F). The images matched the dynamic light scattering data significantly. Our results are consistent with those of previous studies that have reported the synthesis of PdNPs using several biological templates, including extracts of coffee and tea, leaf extracts of *Anacardium occidentale*, *Pulicaria glutinosa*, and *Evolvulus alsinoides*, and saponin.<sup>8,21,35–37</sup>

### Effects of TUB-A and PdNPs on MDA-MB-231 human breast cancer cell viability

WST-8 assay was performed to investigate the cytotoxicity of TUB-A and PdNPs on human breast cancer cells. We first tested the cytotoxic effects of TUB-A and PdNPs, dose dependently. As shown in Figure 2A, significant cytotoxicity was observed from 2 to 20  $\mu$ M concentrations of TUB-A, which showed an IC<sub>50</sub> value of 8  $\mu$ M for 24 h of treatment; when the concentration reached the highest level (10  $\mu$ M), the level of toxicity was higher. Similarly, PdNPs exhibited cytotoxicity against human breast cancer cells with an IC<sub>50</sub> value of 8  $\mu$ M at 24 h (Figure 2B). Both TUB-A and

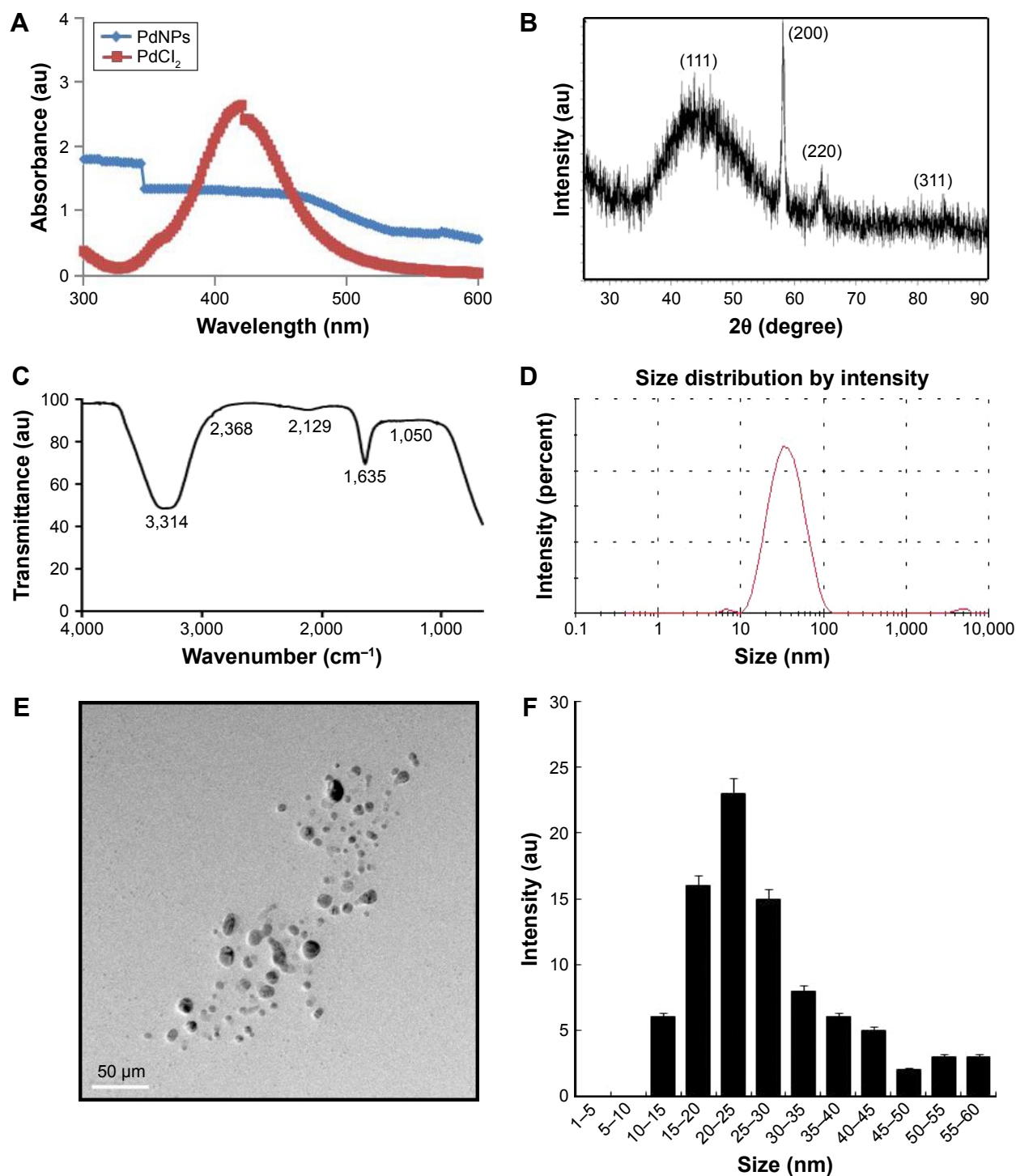


**Figure 1** Synthesis and characterization of PdNPs.

**Notes:** (A) Ultraviolet-visible spectra of PdNPs (blue) and PdCl<sub>2</sub> (red). (B) X-ray diffraction pattern of PdNPs. (C) Fourier-transform infrared spectra of PdNPs. (D) Size distribution analysis of PdNPs by dynamic light scattering. (E) TEM images of PdNPs, (F) Size distributions based on TEM images of PdNPs, ranging from 10 nm to 60 nm.

**Abbreviations:** PdNPs, palladium nanoparticles; PdCl<sub>2</sub>, palladium(II) chloride; TEM, transmission electron microscopy.

PdNPs decreased the cell viability significantly in a dose-dependent manner. Recently, we reported the combinational effect of trichostatin A (TSA) and PdNPs in human breast cancer and HeLa cells, where the IC<sub>50</sub> values

were found to be 200 nM and 300 nM, respectively.<sup>8</sup> The response of any cancer cell line to HDACIs depends on the nature of the HDACI, the concentration and time of exposure, and, importantly, the cell type.<sup>38</sup>

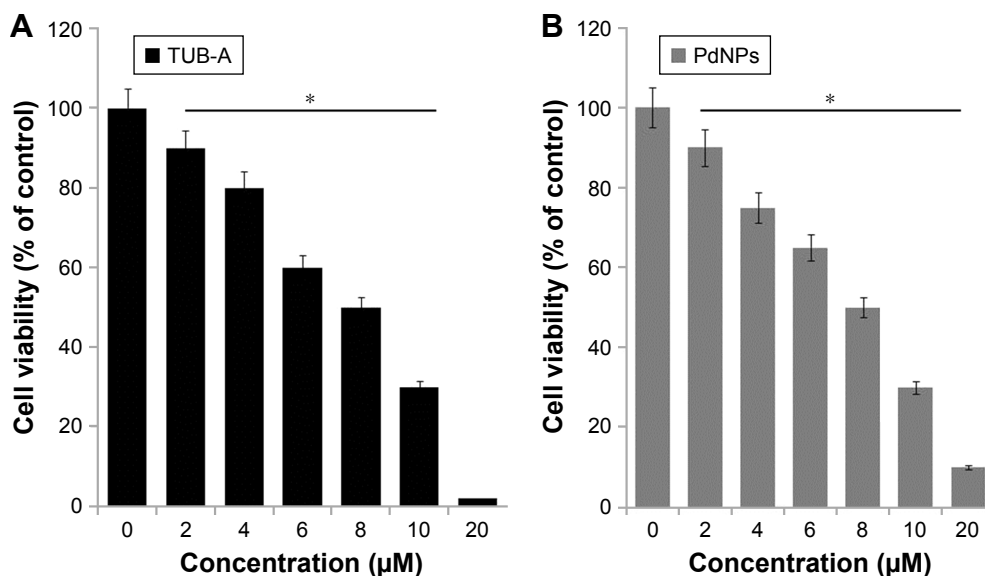


**Figure 2** Dose-dependent effects of TUB-A and PdNPs on cell viability in MDA-MB-231 human breast cancer cells.

**Notes:** MDA-MB-231 human breast cancer cells were incubated with various concentrations of (A) TUB-A (2–20 μM) and (B) PdNPs (2–20 μM) for 24 h. Cell viability was measured by WST-8 assay. The results are expressed as mean ± standard deviation of three separate experiments. The treated groups showed statistically significant differences from the control group, as determined by Student's *t*-test (\**P*<0.05).

**Abbreviations:** TUB-A, tubastatin-A; PdNPs, palladium nanoparticles.

Chang et al<sup>39</sup> studied the differential response of various types of cancer cell lines, including lung cancer, breast cancer, and melanoma cell lines. Their results showed distinct sensitivities of the cells to the pan-inhibitor TSA compared with the class 1 selective inhibitor depsipeptide. For instance, MCF7 cells responded differently to TSA than they did to depsipeptide. Collectively, the results from previous studies and our study conclude that the effect of HDACi on cell viability depends merely on the type of inhibitor as well as the combination reagents. Furthermore, the effectiveness of NPs is dependent on the size, surface chemistry, shape, and type of reducing agents used for their synthesis. Therefore, exploring different sizes of particles derived from various reducing agents is essential for combinatorial therapy. Surprisingly, there are no reports on the effect of TUB-A in human breast cancer cells; therefore, it is necessary to study the effect of TUB-A alone or in combination with PdNPs in all types of cancer cells.

### Effects of TUB-A in combination with PdNPs on MDA-MB-231 human breast cancer cell survival

To determine whether TUB-A interacts with PdNPs, the cytotoxic potency of the combinatorial treatment was measured. Cells were treated with various concentrations of TUB-A (4–10 μM) with 4 μM PdNPs or with various concentrations of PdNPs (4–10 μM) with 4 μM TUB-A. The increasing

concentrations of TUB-A with 4 μM PdNPs significantly inhibited cell survival compared with each drug treatment alone (Figure 3A). Similarly, the increasing concentrations of PdNPs with fixed concentration of TUB-A had an effect comparable to that of increasing the TUB-A concentration, with higher concentrations of TUB-A and PdNPs causing a greater cytotoxic effect (Figure 3B). Notably, 4–10 μM concentration of TUB-A, in combination with 4 μM PdNPs, was particularly effective in inhibiting cell growth. Selection of a low dose of the two reagents is obviously a better strategy to improve anticancer activity and reduce undesired toxicity in cancer cells. Therefore, combinations with various concentrations of TUB-A and PdNPs were investigated to determine the lowest effective concentration of each reagent that would provide the maximum cytotoxic effects. It was established that the cytotoxicity of 4 μM TUB-A combined with 4 μM PdNPs was much more potent in inhibiting cell survival (Figure 3A) than either treatment alone. Therefore, the remaining experiments in cells were carried out with 4 μM of these two reagents, unless otherwise specified. Previous studies have reported that a combination of HDACi, such as TSA combined with curcumin, produced significant anti-proliferative and apoptotic effects compared with either agent alone.<sup>40</sup> The combination of quercetin and TSA significantly increased the cytotoxic effect in A549 cells,<sup>41</sup> whereas that of TSA and PdNPs produced a significant inhibitory effect on cell survival and HDAC activity in HeLa cells.<sup>8</sup>

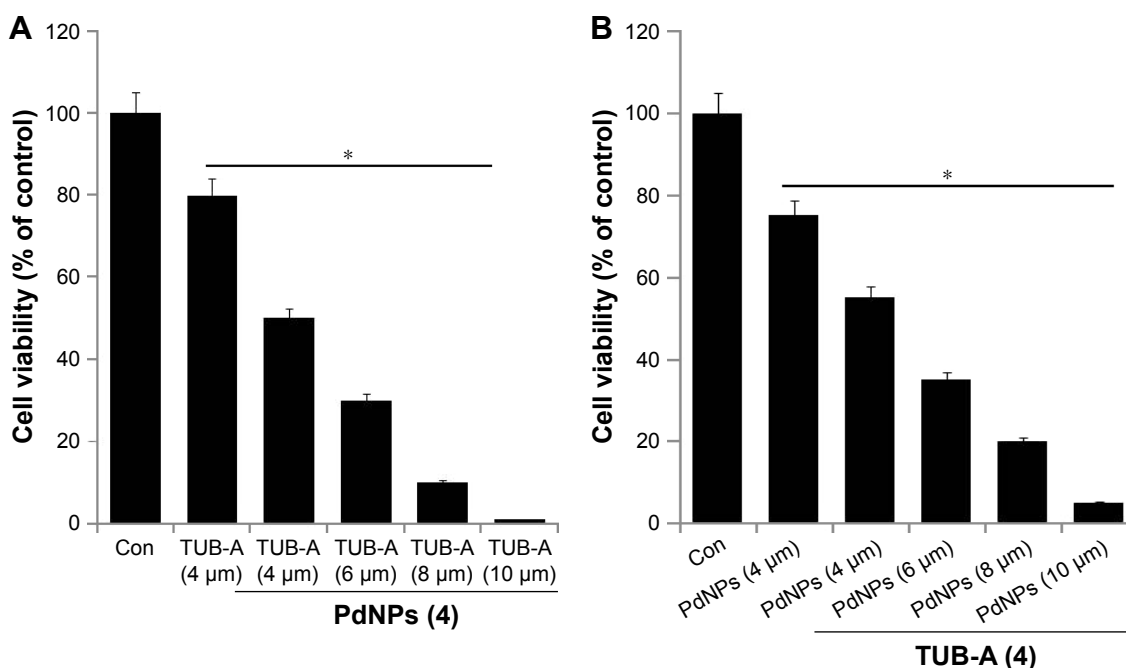


**Figure 3** Effects of increasing concentrations of TUB-A or PdNPs on MDA-MB-231 human breast cancer cells viability.

**Notes:** Human breast cancer cells were coincubated with (A) increasing concentrations of TUB-A (4–10 μM) with 4 μM PdNPs or (B) increasing concentrations of PdNPs (4–10 μM) with 4 μM TUB-A. The results are expressed as mean ± standard deviation of three separate experiments. The treated groups showed statistically significant differences from the control group, as determined by the Student's *t*-test (\**P*<0.05).

**Abbreviations:** Con, control; TUB-A, tubastatin-A; PdNPs, palladium nanoparticles.

## Inhibitory effect of combined TUB-A and PdNPs treatment on cell viability and HDAC activity

In order to determine the correlation between cell viability and HDAC activity, we first evaluated the combinatorial effect of TUB-A and PdNPs on cell viability and HDAC activity in MDA-MB-231 human breast cancer cells. MDA-MB-231 cells treated with TUB-A alone showed a 25% decrease in cell viability, compared with the untreated control, and treatment with PdNPs alone also resulted in a 25% decrease in cell viability relative to the control. On the other hand, the viability of cells treated with TUB-A and PdNPs combined decreased by 70% (Figure 4A). These results indicate and suggest a synergistic effect between TUB-A and PdNPs on MDA-MB-231 cytotoxicity. Zhang et al<sup>42</sup> found that TSA in combination with cisplatin caused a significantly greater inhibitory effect on A549 cells than when given alone. Chao et al reported the potential benefit of vincristine in combination with TUB-A, where vincristine significantly enhanced the cytotoxicity of TUB-A in human acute T-cell lymphoblastic leukemia.<sup>9</sup> Similarly, the combination of vincristine and suberoylanilide hydroxamic acid (SAHA) exhibited greater cytotoxicity (IC<sub>50</sub>, 0.88 nM) than that with each drug alone (IC<sub>50</sub>, 3.3 nM and 840 nM, respectively).

Next, we assessed the levels of HDAC activity in the MDA-MB-231 cell line using HDAC Activity Assay Kit.

To determine the effect of single-drug or combinatorial drug treatment on HDAC activity in vitro, we treated MDA-MB-231 cells with TUB-A (4 μM) and PdNPs (4 μM), or a combination of both, for 24 h. As shown in Figure 4B, TUB-A treatment resulted in significant inhibition (*P*<0.05) of HDAC activity as compared with untreated control cells, and its inhibitory effect was greater than that of PdNPs, indicating the specificity of HDACs. Kaliszczak et al found that the novel small molecule hydroxamate preferentially inhibited HDAC6 activity and tumor growth.<sup>43</sup> Singh et al reported that HDAC activity was significantly inhibited in both A549 and H1299 cells treated with honokiol.<sup>44</sup> HeLa cells treated with TSA and PdNPs exhibited significant inhibition of HDAC activity.<sup>8</sup> The results herein suggest that synthetic HDACs such as TUB-A have promising therapeutic activity, especially in combination with PdNPs. Furthermore, our study provides evidence that the combination of TUB-A and PdNPs suppresses the levels of HDAC activity significantly in MDA-MB-231 cells.

## Effect of combined TUB-A and PdNPs treatment on cell morphology

Morphological changes are an indicator of cell death. The cell morphology of MDA-MB-231 human breast cancer cells was performed after exposure to TUB-A or PdNPs or the combination of both and was studied by light microscopy.



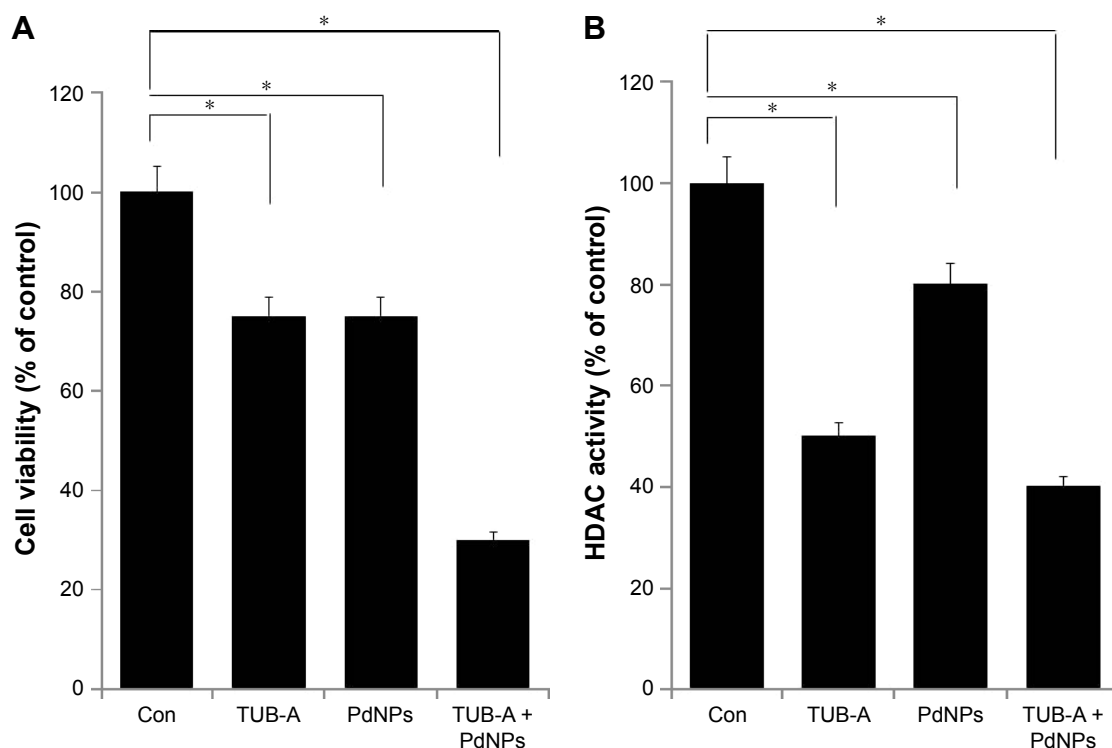


**Figure 4** Effects of combined TUB-A and PdNPs treatment on cell viability and HDAC activity in MDA-MB-231 human breast cancer cells.

**Notes:** Human breast cancer cells were incubated with TUB-A (4  $\mu$ M) and PdNPs (4  $\mu$ M) or a combination of both (at 4  $\mu$ M each) for 24 h. **(A)** Measurement of cell viability by WST-8 assay. **(B)** Measurement of HDAC activity. The results are expressed as mean  $\pm$  standard deviation of three separate experiments. The treated groups showed statistically significant differences from the control group, as determined by Student's *t*-test (\* $P$ <0.05).

**Abbreviations:** Con, control; TUB-A, tubastatin-A; PdNPs, palladium nanoparticles; HDAC, histone deacetylase.

Cells exposed to TUB-A and PdNPs at concentrations of 4  $\mu$ M for 24 h showed distinct morphological changes that indicated that they were unhealthy, whereas cells in the control group appeared normal (Figure 5). The cells exposed to reagents when given alone or in combination appeared to be fragmented and clumped together, exhibiting the severe morphological alterations that would eventually lead to cell death. In addition, the combinatorial treatment produced a higher degree of cell death, observed as cells detached from the plate and with more empty places in the plate. With the exception of the control cells, all the treated samples showed a decrease in the number of cells, particularly those treated with TUB-A and PdNPs combined. Cells became tiny and spherical in shape, forming clusters and eventually detaching from the surface (indicated as brackets in black color in Figure 5). A more pronounced inhibition of cell growth was observed in the combinatorial treatment. In another study, TSA or cisplatin alone or in combination led to marked morphological changes in A549 cells, such as chromatin condensation, nuclear fragmentation, and apoptotic bodies, which are characteristic features of apoptosis.<sup>42</sup> A549 cells treated with either TSA or cisplatin became larger or finger-like, and the cell gap widened. When the cells were treated with TSA combined with cisplatin, the cell density

decreased significantly and cell death increased obviously.<sup>45</sup> Our results are consistent with earlier studies and confirm that the induction of apoptosis is mainly by features such as membrane blebbing, reduced and shrunken cells, condensed

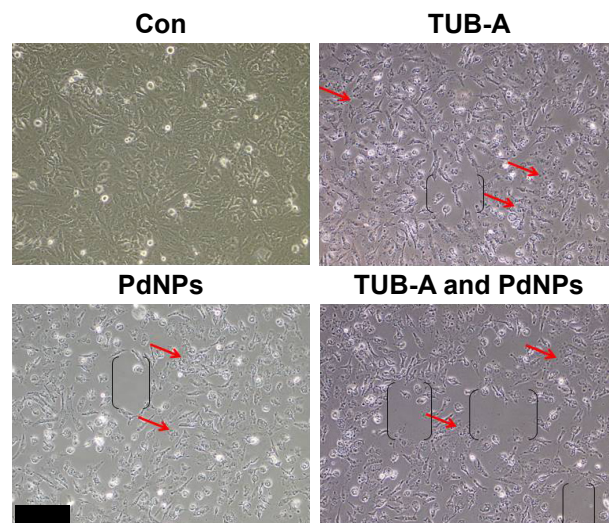


**Figure 5** Effects of TUB-A or PdNPs alone or in combination on cell morphology of MDA-MB-231 human breast cancer cells.

**Notes:** Human breast cancer cells were incubated with TUB-A (4  $\mu$ M) or PdNPs (4  $\mu$ M) or a combination of both (at 4  $\mu$ M each) for 24 h. Red arrows indicate the detachment of cells from the surface. The treated cells were photographed under a light microscope (200  $\mu$ m).

**Abbreviations:** Con, control; TUB-A, tubastatin-A; PdNPs, palladium nanoparticles.

nuclei, and DNA fragmentation.<sup>21,30,46</sup> Collectively, the preliminary data that TUB-A and PdNPs alter cellular morphology provide evidence for their cytotoxicity. The well-established morphological criteria, such as distinct cell shrinkage and membrane blebbing, strongly correlate with apoptotic changes, such as chromatin condensation, nuclear and cell fragmentation, and internucleosomal DNA cleavage.<sup>47</sup> Collectively, these results indicate that cell detachment and loss of viability are attributable to the enhanced inhibitory activity of TUB-A and PdNPs combined in breast cancer cells.

### Effect of combined TUB-A and PdNPs treatment on cytotoxicity in MDA-MB-231 human breast cancer cells

LDH leakage assay is crucial for the determination of cytotoxicity in any type of cells subjected to cytotoxic treatments. Therefore, we examined LDH leakage in MDA-MB-231 cells exposed to TUB-A or PdNPs or a combination of both. The results clearly suggest that both TUB-A- and PdNPs-treated cells showed significant LDH leakage, and the combination of both enhanced the leakage effect even more (Figure 6A). Previous studies also demonstrated that TSA alone increased LDH leakage in primary hepatic stellate cells.<sup>48</sup> Recently, we observed that the combination of TSA and PdNPs increased LDH leakage over that of single-drug treatment in HeLa cells.<sup>8</sup>

Carew et al reported that HDACI treatment results in ROS production.<sup>49</sup> ROS are the ultimate key players of HDACI-induced apoptosis in cancer cells, and their generation plays an important role in HDACI-induced cell death.<sup>50</sup> The role of TUB-A and the potentiation of PdNPs enhancement on ROS production are still not clear. Therefore, we investigated the ROS-related effects of these two drugs alone or in combination, on MDA-MB-231 cells for 24 h. The results revealed a pronounced increase in ROS levels, reflected by the oxidation-sensitive dye H<sub>2</sub>DCFDA. Significantly, TUB-A or PdNPs administered alone did induce the generation of ROS, but the combination of both showed a greater effect (Figure 6B). Vorinostat was shown to induce ROS and DNA damage in a number of tumor types.<sup>51</sup> The present findings provide evidence that early TUB-A-mediated ROS generation plays a critical role in sensitizing human breast cancer cells to PdNPs-induced cell death. Our results are in line with previous studies that had demonstrated that ROS accumulation in transformed cells exposed to structurally diverse HDACIs, including vorinostat, TSA, sodium butyrate, MS275, and LAQ-824, is responsible for the lethality of these inhibitors.<sup>8,52–55</sup>

### Effects of TUB-A and PdNPs on oxidative stress markers

Several studies have suggested that various types of NPs induce cytotoxicity in cancer cells via the production of ROS,

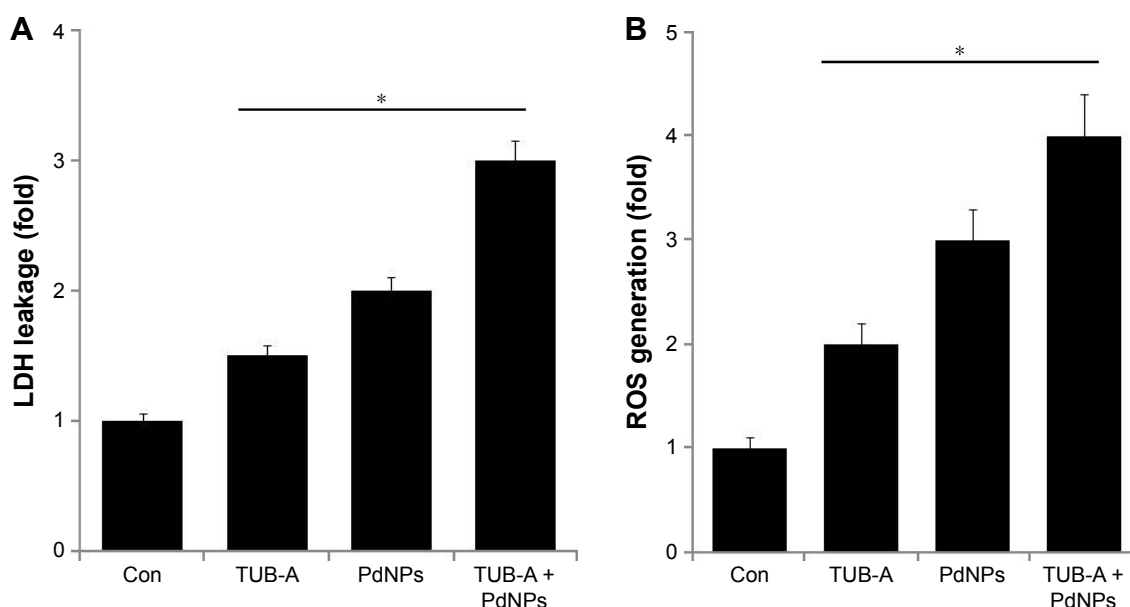


**Figure 6** Cytotoxicity effects of TUB-A or PdNPs alone or in combination on MDA-MB-231 human breast cancer cells.

**Notes:** The cells were treated with TUB-A (4  $\mu$ M), PdNPs (4  $\mu$ M), or a combination of both (at 4  $\mu$ M each) for 24 h. **(A)** Lactate dehydrogenase (LDH) activity was measured at 490 nm, using LDH cytotoxicity kit (Sigma-Aldrich, St Louis, MO, USA). **(B)** Reactive oxygen species (ROS) was measured (as the relative fluorescence of 2',7'-dichlorofluorescein) with a spectrofluorometer. The results are expressed as mean  $\pm$  standard deviation of three separate experiments. The treated groups showed statistically significant differences from the control group, as determined by Student's *t*-test ( $*P < 0.05$ ).

**Abbreviations:** Con, control; TUB-A, tubastatin-A; PdNPs, palladium nanoparticles.

which in turn leads to cellular damage and cell death.<sup>21,31</sup> Oxidative stress refers to the imbalance between pro-oxidant and antioxidant levels in favor of pro-oxidants in cells and tissues, which could modify the status of several biomolecules, such as lipids, proteins, and DNA. Such modifications or damage to these molecules are called oxidative damage.<sup>56</sup> Oxidative stress is a critical factor in HDACI-induced cell death.<sup>57</sup> Biomarkers of oxidative stress could interact with ROS in the microenvironment and with molecules of the antioxidant system that change in response to increased redox stress. MDA is generated via peroxidation of polyunsaturated fatty acids.<sup>58</sup> We determined the level of MDA in single-drug treatment as well as in combinatorial treatment of TUB-A and PdNPs in MDA-MB-231 cells (Figure 7A). The results clearly indicated that the combinatorial treatment had a more significant effect (2.7 nmol/mg of protein) on MDA-MB-231 cells than single treatment with either TUB-A (1 nmol/mg of protein) or PdNPs (1.7 nmol/mg of protein). Previous reports showed that HDACIs such as TSA and PdNPs induced a remarkable increase of MDA in human ovarian cancer and HeLa cells.<sup>8,21</sup>

The changes in the intracellular GSH levels were likewise investigated by treating MDA-MB-231 cells with either TUB-A or PdNPs alone or in combination, where all treatments showed a decrease in GSH compared with untreated cells (Figure 7B). The single or combinatorial treatment also decreased the intracellular SOD and CAT levels (Figure 7C and D). Similarly, HeLa cells treated with suberoyl bis-hydroxamic acid (SBHA) and TSA showed a lower level of antioxidants.<sup>8,59</sup> It is known that the intracellular GSH content has a decisive effect on anticancer drug-induced apoptosis, where apoptotic effects are inversely related to the GSH content.<sup>60–62</sup> Furthermore, You and Park clearly demonstrated that the reduction in GSH level is responsible not only for cell death but also for increased ROS levels in SBHA-treated HeLa cells.<sup>59</sup> SBHA decreased the levels of CAT, Cu/ZnSOD, and especially MnSOD, the latter of which is located in mitochondria and catalyzes the dismutation of superoxide into oxygen and hydrogen peroxide.<sup>59,63</sup> Similarly, Zhang et al<sup>8</sup> observed decreased levels of GSH, SOD, and CAT in TSA-treated or combination of TSA and PdNPs-treated human cervical cancer cells.

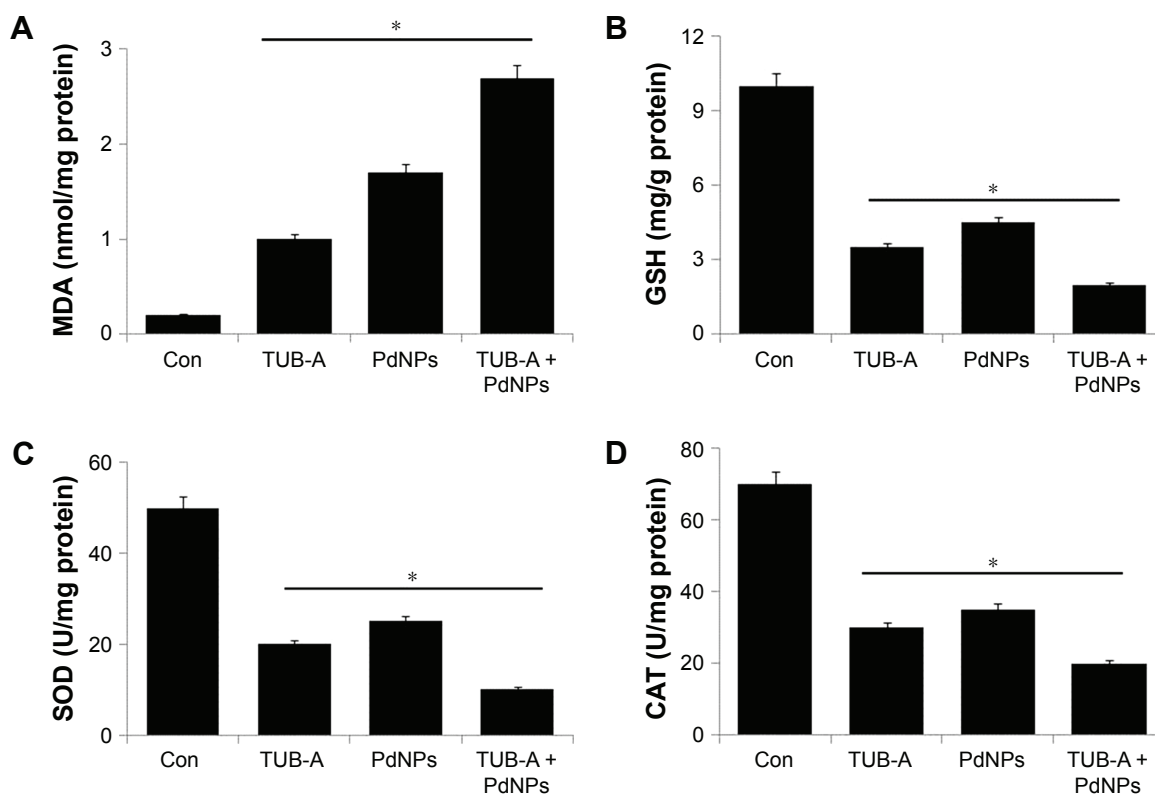


**Figure 7** Effects of TUB-A, PdNPs, or a combination of both on oxidative stress markers in MDA-MB-231 human breast cancer cells.

**Notes:** (A) The cells were treated with TUB-A (4  $\mu$ M), PdNPs (4  $\mu$ M), or a combination of both (at 4  $\mu$ M each) for 24 h. After incubation, the cells were harvested, washed twice with ice-cold PBS, and then disrupted by ultrasonication for 5 min on ice. The concentration of malondialdehyde (MDA) was expressed as nanomole per milligram of protein. (B) The concentration of glutathione (GSH) was expressed as milligram per gram of protein. (C) The specific activity of superoxide dismutase (SOD) was expressed as unit per milligram of protein. (D) The specific activity of catalase (CAT) was expressed as unit per milligram of protein. The results are expressed as mean  $\pm$  standard deviation of three independent experiments. The treated cells showed statistically significant differences from the untreated cells, as determined by the Student's *t*-test (\* $P$ <0.05).

**Abbreviations:** Con, control; TUB-A, tubastatin-A; PdNPs, palladium nanoparticles.

## Effects of combined TUB-A and PdNPs treatment on the MMP and caspase-3 activity

Mitochondria play a crucial role in both the intrinsic and extrinsic apoptotic pathways.<sup>9</sup> ATP synthesis is mainly carried out by the transmembrane electrochemical gradient produced by the mitochondrial respiratory chain, which is the vital site of ROS production and hence a major source of ROS.<sup>64</sup> Dissipation of  $\Delta\Psi_m$  is believed to be a key upstream event during apoptosis. To test whether the TUB-A/PdNPs-mediated apoptotic pathway is associated with mitochondrial function, changes in the mitochondrial transmembrane potential were assessed by applying a membrane-permeable lipophilic cationic dye. As shown in Figure 8A, treatment with TUB-A or PdNPs alone was sufficient to affect  $\Delta\Psi_m$ , and this phenomenon was enhanced by the combinatorial treatment. It has been shown that HDACIs can induce apoptosis by several mechanisms in a variety of cancer cells. HDACIs induced mitochondrial membrane damage with concomitant cytochrome *c* release as well as apoptosis in a T-cell leukemia

cell line and in various type I and type II endometrial cancers, including Ark2, Ishikawa, and AN3 cell lines.<sup>65,66</sup>

As mentioned previously, HDACIs activate the mitochondrial apoptotic pathway by releasing cytochrome *c* from the mitochondrial intermembrane space and activating caspase-3.<sup>67</sup> Therefore, to further characterize the specific apoptotic pathways activated by TUB-A and PdNPs, we measured caspase-3 activity in cells that were subjected to single or combined drug treatment for 24 h, in the presence or absence of a caspase-3 inhibitor. The combination of TUB-A and PdNPs induced a significantly higher level of caspase-3 activity than did the single-drug treatments. This indicated that the combinatorial treatment could promote caspase-3-mediated cell death (Figure 8B). SAHA alone also significantly induced caspase-3 expression in MDA-MB-231, but not MCF7, cells. Tumor necrosis factor-related apoptosis-inducing ligand (TRAIL) alone and combined TRAIL and SAHA treatment likewise significantly induced caspase-3 in MDA-MB-231 cells.<sup>68</sup> Okada et al found that the combination of 5-fluorouracil and depsipeptide sensitized

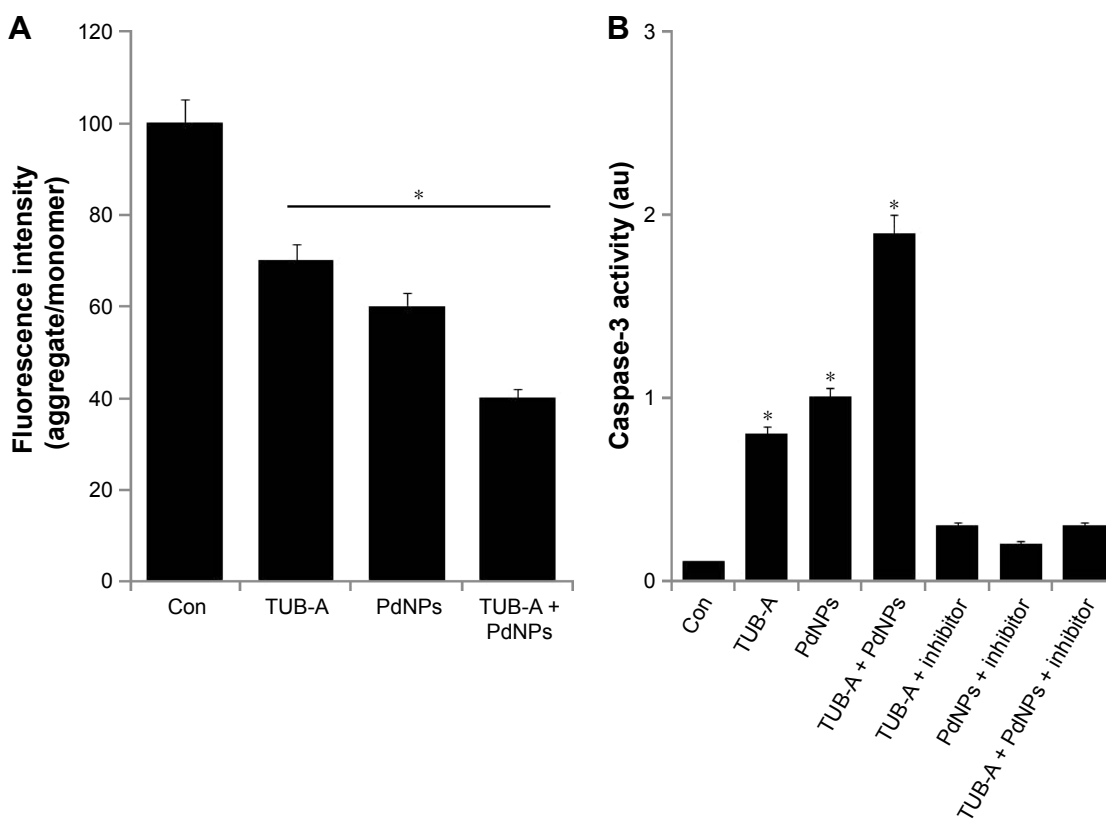


**Figure 8** Effects of TUB-A, PdNPs, or a combination of both on the mitochondrial membrane potential and caspase-3 activity.

**Notes:** The cells were treated with TUB-A (4  $\mu$ M), PdNPs (4  $\mu$ M), or a combination of both (at 4  $\mu$ M each) for 24 h. **(A)** Determination of  $\Delta\Psi_m$  (ratio of JC-1 aggregate to monomer) in treated breast cancer cells. **(B)** Cells treated with TUB-A (4  $\mu$ M), PdNPs (4  $\mu$ M), or a combination of both (at 4  $\mu$ M each) for 24 h, with and without caspase inhibitor. The concentration of P-nitroanilide released from the substrate was calculated from the absorbance at 405 nm. The results are expressed as mean  $\pm$  standard deviation of three separate experiments. The treated groups showed statistically significant differences from the control group, as determined by Student's *t*-test (\* $P$ <0.05).

**Abbreviations:** Con, control; TUB-A, tubastatin-A; PdNPs, palladium nanoparticles.

human colon cancer HCT-116, HT29, and SW48 cells toward apoptosis induction by caspase-3/-7 activation.<sup>69</sup> Collectively, the present study and results from previous studies suggest that HDACIs like TUB-A potentiate the effects of PdNPs in caspase-3 activation, which is the underlying mechanism of the apoptosis effect. It clearly suggests that both TUB-A and PdNPs induce caspase-3-dependent apoptosis in MDA-MB-231 cells.

### Induction of apoptosis in MDA-MB-231 cells by combined TUB-A and PdNPs treatment

Caspases mainly drive apoptotic signaling and execute cell death. Chemotherapeutic agents and UV irradiation cause the release of mitochondrial cytochrome *c*, which then binds to apoptotic protease activating factor 1. This complex, along with adenine nucleotides, promotes caspase-9 autoactivation. The activated caspase-9 in turn activates executioner caspases, such as caspases-3, -6, and -7.<sup>70</sup> Caspase-3 is the primary inducer of apoptotic internucleosomal DNA fragmentation.<sup>71</sup> In order to determine the level of caspase-3-mediated DNA fragmentation in MDA-MB-231 cells, the cells were treated with TUB-A or PdNPs or a combination of both for 24 h, and then TUNEL assay was performed. The appearance of TUNEL-positive cells was more significant in the treated cells than in the untreated controls (Figure 9). Again, the combined drug treatment stimulated a greater level of apoptosis than the single-drug treatments. Our results are consistent with that of a previous study, in which TSA and sodium butyrate induced apoptosis in thymocytes in a concentration-dependent manner via DNA fragmentation, increased chromatin relaxation, and enhanced DNA accessibility.<sup>72</sup> Kaliszczak et al found that the novel small molecule C1A could inhibit HDAC activity, induce apoptosis, and inhibit proliferation of a panel of human tumor cell lines, as well as activate caspase-3 expression in vivo with subsequent fragmented DNA staining (TUNEL) increases of six- and seven-fold.<sup>43</sup> The HDACI honokiol inhibited the growth of both A549 and H1299 cells, and tumor cells from honokiol-treated mice were shown to undergo apoptotic cell death, as indicated by the TUNEL-positive cells as well as increases in the levels of pro-apoptotic Bax protein and cleaved caspase-3.<sup>44</sup> A549 cells treated with the combination of TSA and cisplatin showed significantly more chromatin condensation, nuclear fragmentation, and apoptotic bodies than did cells in the single-drug treatment group.<sup>45</sup> Altogether, these results suggest that combined TUB-A and PdNPs treatment induces cell death mediated by caspase activation and DNA fragmentation.

### Effects of combined TUB-A and PdNPs treatment on the expression of apoptotic genes

Generally, HDACIs could affect transcription by inducing acetylation of histones, transcription factors, and other proteins that regulate transcription.<sup>73–76</sup> HDACIs are known to activate both extrinsic and intrinsic apoptotic pathways, which are initiated through death receptors on the cell surface and through mitochondria, respectively. The intrinsic apoptotic pathway is the major pathway through which HDACIs induce cell death.<sup>38</sup> Previously, several studies suggested that HDACIs could upregulate pro-apoptotic proteins of the Bcl-2 family (eg, Bim, Bmf, Bax, Bak, and Bik)<sup>77–79</sup> and downregulate anti-apoptotic proteins of the Bcl-2 family (eg, Bcl-2, Bcl-XL, Bcl-w, and Mcl-1).<sup>78–80</sup> To determine the effect of TUB-A or PdNPs or a combination of both on the expression of apoptotic and anti-apoptotic genes, we measured the expression levels of p53, Bax, Bak, Bcl-2, caspase-3, and caspase-9 using RT-PCR. TUB-A clearly upregulated p53, Bax, Bak, caspase-3, and caspase-9, whereas PdNPs were more effective in upregulating p53, Bax, Bak, Bcl-2, caspase-3, and caspase-9 (Figure 10). Interestingly, the combinatorial treatment showed a significant 3–4-fold higher effect in all the genes tested. It is known that in mitochondria, the release of mitochondrial intermembrane proteins, such as cytochrome *c*, apoptosis-inducing factor, and Smac, leads to the activation of caspases.<sup>81</sup> However, the effects of HDACIs in increasing the pro-apoptotic proteins and decreasing the anti-apoptotic proteins are cell-type dependent.<sup>79</sup> Xu et al found that the basal levels of both pro- and anti-apoptotic proteins were significantly different in different tumor cells, even in the same type of cancer.<sup>79</sup> Our results are in line with a previous report that demonstrated the combination of SBHA and a proteasome inhibitor to significantly increase the expression of p53, Bax, Bcl-xS, and Bak protein levels and decrease the Bcl-2 level in MCF7 and MDA-MB-231 cells.<sup>82</sup> Moreover, the human renal cell carcinoma line Caki, treated with TSA and TRAIL, showed increased expression of caspase-3, -8, and -9.<sup>83</sup> Chao et al<sup>9</sup> observed that when T-cell leukemic cells were treated with vincristine and SAHA combined, caspase-3 and -6 to -9 and poly (ADP-ribose) polymerase were synergistically induced, suggesting that the combinatorial treatment activates both the intrinsic and extrinsic apoptotic pathways. Overall, TUB-A-induced apoptosis was greatly enhanced in the presence of PdNPs, suggesting that apoptosis-inducing NPs like PdNPs play an important role in the efficacy of TUB-A. Interestingly, TUB-A enhanced PdNPs-induced cell death in the

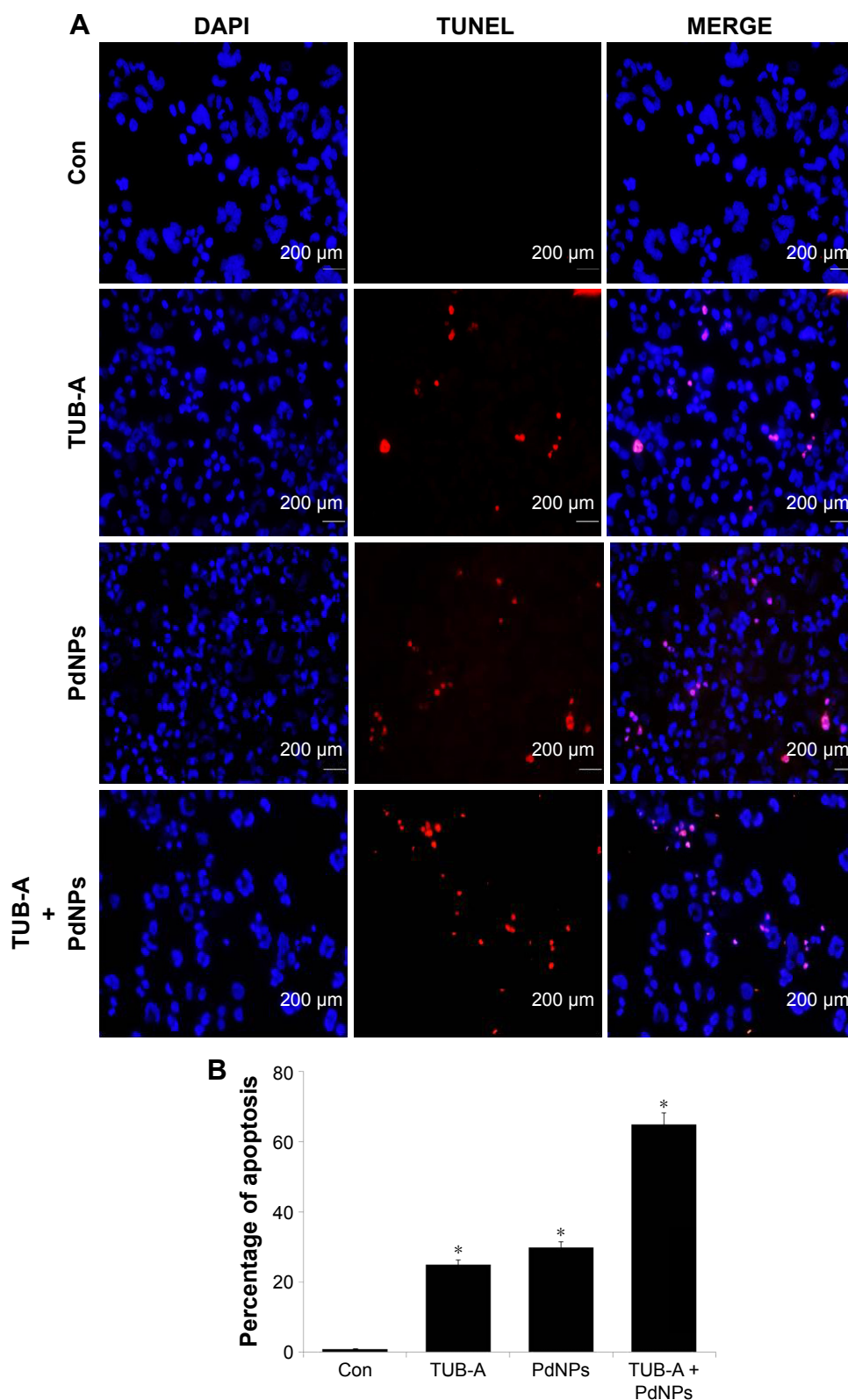


**Figure 9** Effects of TUB-A, PdNPs, or a combination of both on apoptosis.

**Notes:** (A) The cells were treated with TUB-A (4  $\mu$ M), PdNPs (4  $\mu$ M), or a combination of both (at 4  $\mu$ M each) for 24 h. Apoptosis was assessed by TUNEL assay; the nuclei were counterstained with DAPI. Representative images show apoptotic (fragmented) DNA (red stained) and the corresponding cell nuclei (blue stained). (B) The percentage of apoptosis was calculated in cells treated with TUB-A (4  $\mu$ M), PdNPs (4  $\mu$ M), or a combination of both (at 4  $\mu$ M each) for 24 h using TUNEL. \* $p$ <0.05.

**Abbreviations:** Con, control; TUB-A, tubastatin-A; PdNPs, palladium nanoparticles; TUNEL, terminal deoxynucleotidyl transferase dUTP nick end labeling.

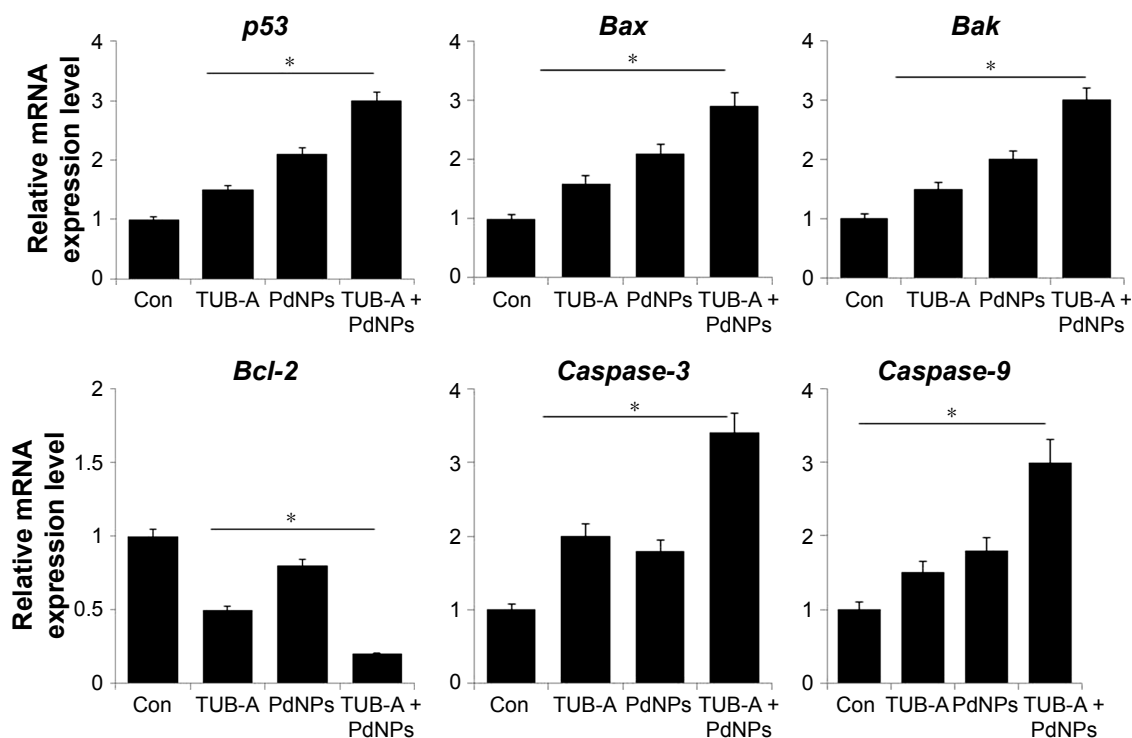


**Figure 10** Effect of combined TUB-A and PdNPs treatment on the expression of apoptotic genes.

**Notes:** The cells were treated with TUB-A (4  $\mu$ M), PdNPs (4  $\mu$ M), or a combination of both (at 4  $\mu$ M each) for 24 h, and then the relative expression levels of pro-apoptotic and anti-apoptotic genes were analyzed by qRT-PCR. The results are expressed as mean  $\pm$  standard deviation of three separate experiments. The treatment groups showed statistically significant differences from the control group, as determined by Student's *t*-test (\* $P < 0.05$ ).

**Abbreviations:** Con, control; TUB-A, tubastatin-A; PdNPs, palladium nanoparticles.

MDA-MB-231 human breast cancer cell line by regulating many pro-apoptotic genes, including *p53*, *Bax*, *Bak*, *Bcl-2*, *caspase-3*, and *caspase-9*.

## Conclusion

Because drug resistance is a common problem in cancer therapy, it is necessary to identify alternative therapeutic approaches for cancer. In this regard, combinatorial therapy is a suitable therapeutic strategy for minimizing drug resistance. To explore this option, we synthesized PdNPs, using the novel biomolecule RPE. The synthesized PdNPs were spherical in shape with an average size of 25 nm. We examined the effect of PdNPs in combination with TUB-A on MDA-MB-231 cells, using various cellular assays. The results obtained from this study suggest that the combination of TUB-A and PdNPs synergistically induces apoptosis by decreasing cell viability and inhibiting HDAC activity. Furthermore, the synergistic effect was more significant in cytotoxicity, loss of  $\Delta\Psi_m$ , and increases of caspase-3 activity, DNA fragmentation, and expression of pro-apoptotic genes. The results from this study strongly suggest a strong synergistic interaction between PdNPs and TUB-A

in human breast cancer cells. Collectively, our data suggest that the combination of TUB-A and PdNPs could provide a novel and effective and possible supplemental treatment for breast cancer patients. Therefore, this combination of PdNPs and TUB-A is of great promise in the treatment of breast cancer. The combination of PdNPs and TUB-A contains nanoparticles, and TUB-A could reduce toxicity, enhance efficacy, and overcome drug resistance and sustained treatment responses in cancer patients. However, further investigations are required to elucidate the molecular mechanism of apoptosis induced by TUB-A and PdNPs. Many parallel studies are also required to compare several HDACi in combination with standard chemotherapies or targeted therapies to identify the most effective and safe combinations.

## Acknowledgments

This study was supported by the KU-Research Professor Program of Konkuk University. This study was also supported by the Priority Academic Program Development of Jiangsu Higher Education Institutions (PAPD), and China Postdoctoral Science Foundation (2015M571827/1402001C).

## Disclosure

The authors report no conflicts of interest in this work.

## References

- Alberghina L, Chiaradonna F, Vanoni M. Systems biology and the molecular circuits of cancer. *Chembiochem*. 2004;5(10):1322–1333.
- Fearon ER. Human cancer syndromes: clues to the origin and nature of cancer. *Science*. 1997;278(5340):1043–1050.
- Vogelstein B, Kinzler KW. Cancer genes and the pathways they control. *Nat Med*. 2004;10(8):789–799.
- Siegel RL, Miller KD, Jemal A. Cancer statistics, 2015. *CA Cancer J Clin*. 2015;65(1):5–29.
- American Cancer Society, Inc. *Breast Cancer Facts & Figures 2015–2016*. Atlanta: American Cancer Society, Inc.; 2015.
- Olszewski U, Hamilton G. A better platinum-based anticancer drug yet to come? *Anticancer Agents Med Chem*. 2010;10(4):293–301.
- Diyabalanage HV, Granda ML, Hooker JM. Combination therapy: histone deacetylase inhibitors and platinum-based chemotherapeutics for cancer. *Cancer Lett*. 2013;329(1):1–8.
- Zhang XF, Yan Q, Shen W, Gurunathan S. Trichostatin A enhances the apoptotic potential of palladium nanoparticles in human cervical cancer cells. *Int J Mol Sci*. 2016;17(8):pii:E1354.
- Chao MW, Lai MJ, Liou JP, et al. The synergic effect of vincristine and vorinostat in leukemia in vitro and in vivo. *J Hematol Oncol*. 2015;8:82.
- Thurn K, Thomas S, Raha P, Qureshi I, Munster PN. Inhibition of class I histone deacetylases attenuates anthracycline induced activation of the ATM pathway. *Cancer Res*. 2011;71(8 Suppl):Abstract 2614.
- Petrucelli LA, Dupere-Richer D, Pettersson F, Retrouvey H, Skoulikas S, Miller WH Jr. Vorinostat induces reactive oxygen species and DNA damage in acute myeloid leukemia cells. *PLoS One*. 2011;6(6):e20987.
- Okada M, Lee L, Maekawa R, et al. Epigenetic changes of the Cyp11a1 promoter region in granulosa cells undergoing luteinization during ovulation in female rats. *Endocrinology*. 2016;157(9):3344–3354.
- Rosik L, Niegisch G, Fischer U, Jung M, Schulz WA, Hoffmann MJ. Limited efficacy of specific HDAC6 inhibition in urothelial cancer cells. *Cancer Biol Ther*. 2014;15(6):742–757.
- Mishra SK, Mandal M, Mazumdar A, Kumar R. Dynamic chromatin remodeling on the HER2 promoter in human breast cancer cells. *FEBS Lett*. 2001;507(1):88–94.
- Arifin JK, das Gupta K, Kapetanovic R, et al. Histone deacetylase inhibitors promote mitochondrial reactive oxygen species production and bacterial clearance by human macrophages. *Antimicrob Agents Chemother*. 2015;60(3):1521–1529.
- Falkenberg KJ, Johnstone RW. Histone deacetylases and their inhibitors in cancer, neurological diseases and immune disorders. *Nat Rev Drug Discov*. 2014;13(9):673–691.
- Li Z, Zhu WG. Targeting histone deacetylases for cancer therapy: from molecular mechanisms to clinical implications. *Int J Biol Sci*. 2014;10(7):757–770.
- Zhang J, Zhong Q. Histone deacetylase inhibitors and cell death. *Cell Mol Life Sci*. 2014;71(20):3885–3901.
- Davis ME, Chen Z, Shin DM. Nanoparticle therapeutics: an emerging treatment modality for cancer. *Nat Rev Drug Discov*. 2008;7(9):771–782.
- Gurunathan S, Han JW, Eppakayala V, Jeyaraj M, Kim JH. Cytotoxicity of biologically synthesized silver nanoparticles in MDA-MB-231 human breast cancer cells. *Biomed Res Int*. 2013;2013:535796.
- Gurunathan S, Kim E, Han JW, Park JH, Kim JH. Green chemistry approach for synthesis of effective anticancer palladium nanoparticles. *Molecules*. 2015;20(12):22476–22498.
- Wu XJ, Zhou LZ, Su Y, Dong CM. An autoreduction method to prepare plasmonic gold-embedded polypeptide micelles for synergistic chemo-photothermal therapy. *J Mater Chem B*. 2016;4(12):2142–2152.
- Cookson J. The Preparation of Palladium Nanoparticles. *Platin Met Rev*. 2012;56(2):83–98.
- Astruc D. Palladium nanoparticles as efficient green homogeneous and heterogeneous carbon-carbon coupling precatalysts: a unifying view. *Inorg Chem*. 2007;46(6):1884–1894.
- Semagina N, Renken A, Kiwi-Minsker L. Palladium nanoparticle size effect in 1-hexyne selective hydrogenation. *J Phys Chem C*. 2007;111(37):13933–13937.
- Dimitratos N, Porta F, Prati L, Villa A. Synergetic effect of platinum or palladium on gold catalyst in the selective oxidation of D-sorbitol. *Catal Lett*. 2005;99(3–4):181–185.
- Beller M, Fischer H, Kühlein K, Reisinger CP, Herrmann WA. First palladium-catalyzed Heck reactions with efficient colloidal catalyst systems. *J Organomet Chem*. 1996;520(1–2):257–259.
- Cheong SS, Watt JD, Tilley RD. Shape control of platinum and palladium nanoparticles for catalysis. *Nanoscale*. 2010;2(10):2045–2053.
- Anh TD, Ahn MY, Kim SA, Yoon JH, Ahn SG. The histone deacetylase inhibitor, trichostatin A, induces G2/M phase arrest and apoptosis in YD-10B oral squamous carcinoma cells. *Oncol Rep*. 2012;27(2):455–460.
- Gurunathan S, Jeong JK, Han JW, Zhang XF, Park JH, Kim JH. Multidimensional effects of biologically synthesized silver nanoparticles in *Helicobacter pylori*, *Helicobacter felis*, and human lung (L132) and lung carcinoma A549 cells. *Nanoscale Res Lett*. 2015;10:35.
- Gurunathan S, Raman J, Malek NA, John PA, Vikineswary S. Green synthesis of silver nanoparticles using *Ganoderma neo-japonicum* Imazeki: a potential cytotoxic agent against breast cancer cells. *Int J Nanomed*. 2013;8:4399–4413.
- Mahdieh M, Zolanvari A, Azimee AS, Mahdieh M. Green biosynthesis of silver nanoparticles by *Spirulina platensis*. *Sci Iran*. 2012;19(3):926–929.
- Patel V, Berthold D, Puranik P, Gantar M. Screening of cyanobacteria and microalgae for their ability to synthesize silver nanoparticles with antibacterial activity. *Biotechnol Rep*. 2015;5:112–119.
- Bekasova OD, Brekhovskikh AA, Revina AA, Dubinchuk VT. Preparation and optical properties of silver nanoparticles in R-phycoerythrin, a protein matrix. *Inorg Mater*. 2008;44(8):835–841.
- Sheny DS, Philip D, Mathew J. Rapid green synthesis of palladium nanoparticles using the dried leaf of *Anacardium occidentale*. *Spectrochim Acta A Mol Biomol Spectrosc*. 2012;91:35–38.
- Khan M, Khan M, Kuniyil M, et al. Biogenic synthesis of palladium nanoparticles using *Pulicaria glutinosa* extract and their catalytic activity towards the Suzuki coupling reaction. *Dalton Trans*. 2014;43(24):9026–9031.
- Nadagouda MN, Varma RS. Green synthesis of silver and palladium nanoparticles at room temperature using coffee and tea extract. *Green Chem*. 2008;10(8):859–862.
- Xu WS, Parmigiani RB, Marks PA. Histone deacetylase inhibitors: molecular mechanisms of action. *Oncogene*. 2007;26(37):5541–5552.
- Chang J, Varghese DS, Gillam MC, et al. Differential response of cancer cells to HDAC inhibitors trichostatin A and depsipeptide. *Br J Cancer*. 2012;106(1):116–125.
- Yan G, Eller MS, Elm C, et al. Selective inhibition of p300 HAT blocks cell cycle progression, induces cellular senescence, and inhibits the DNA damage response in melanoma cells. *J Invest Dermatol*. 2013;133(10):2444–2452.
- Chan ST, Yang NC, Huang CS, Liao JW, Yeh SL. Quercetin enhances the antitumor activity of trichostatin A through upregulation of p53 protein expression in vitro and in vivo. *PLoS One*. 2013;8(1):e54255.
- Zhang YW, Zheng Y, Wang JZ, et al. Integrated analysis of DNA methylation and mRNA expression profiling reveals candidate genes associated with cisplatin resistance in non-small cell lung cancer. *Epigenetics*. 2014;9(6):896–909.
- Kaliszczak M, Trousil S, Aberg O, Perumal M, Nguyen QD, Aboagye EO. A novel small molecule hydroxamate preferentially inhibits HDAC6 activity and tumour growth. *Br J Cancer*. 2013;108(2):342–350.
- Singh T, Prasad R, Katiyar SK. Inhibition of class I histone deacetylases in non-small cell lung cancer cells by honokiol leads to suppression of cancer cell proliferation and induction of cell death in vitro and in vivo models. *Epigenetics*. 2013;8(1):54–65.



45. Zhang X, Jiang SJ, Shang B, Jiang HJ. Effects of histone deacetylase inhibitor trichostatin A combined with cisplatin on apoptosis of A549 cell line. *Thorac Cancer*. 2015;6(2):202–208.
46. Netala VR, Bethu MS, Pushpalatha B, et al. Biogenesis of silver nanoparticles using endophytic fungus *Pestalotiopsis microspora* and evaluation of their antioxidant and anticancer activities. *Int J Nanomedicine*. 2016;11:5683–5696.
47. Naora H, Nishida T, Shindo Y, Adachi M, Naora H. Constitutively enhanced nbl expression is associated with the induction of internucleosomal DNA cleavage by actinomycin D. *Biochem Biophys Res Commun*. 1996;224(1):258–264.
48. Niki T, Rombouts K, De Bleser P, et al. A histone deacetylase inhibitor, trichostatin A, suppresses myofibroblastic differentiation of rat hepatic stellate cells in primary culture. *Hepatology*. 1999;29(3):858–867.
49. Carew JS, Giles FJ, Nawrocki ST. Histone deacetylase inhibitors: mechanisms of cell death and promise in combination cancer therapy. *Cancer Lett*. 2008;269(1):7–17.
50. Rosato RR, Grant S. Histone deacetylase inhibitors: insights into mechanisms of lethality. *Expert Opin Ther Targets*. 2005;9(4):809–824.
51. Rahmani M, Reese E, Dai Y, Bauer C, Payne SG, et al. Coadministration of histone deacetylase inhibitors and perifosine synergistically induces apoptosis in human leukemia cells through Akt and ERK1/2 inactivation and the generation of ceramide and reactive oxygen species. *Cancer Res*. 2005;65:2422–2432.
52. Louis M, Rosato RR, Brault L, et al. The histone deacetylase inhibitor sodium butyrate induces breast cancer cell apoptosis through diverse cytotoxic actions including glutathione depletion and oxidative stress. *Int J Oncol*. 2004;25(6):1701–1711.
53. Rosato RR, Almenara JA, Grant S. The histone deacetylase inhibitor MS-275 promotes differentiation or apoptosis in human leukemia cells through a process regulated by generation of reactive oxygen species and induction of p21 (CIP1/WAF1). *Cancer Res*. 2003;63(13):3637–3645.
54. Rosato RR, Almenara JA, Maggio SC, et al. Role of histone deacetylase inhibitor-induced reactive oxygen species and DNA damage in LAQ-824/fludarabine antileukemic interactions. *Molecular Cancer Ther*. 2008;7(10):3285–3297.
55. Ruefli AA, Ausserlechner MJ, Bernhard D, et al. The histone deacetylase inhibitor and chemotherapeutic agent suberoylanilide hydroxamic acid (SAHA) induces a cell-death pathway characterized by cleavage of Bid and production of reactive oxygen species. *PNatl Acad Sci U S A*. 2001;98(19):10833–10838.
56. Kalyanaram B. Teaching the basics of redox biology to medical and graduate students: oxidants, antioxidants and disease mechanisms. *Redox Biol*. 2013;1(1):244–257.
57. Ungerstedt JS, Sowa Y, Xu WS, et al. Role of thioredoxin in the response of normal and transformed cells to histone deacetylase inhibitors. *Proc Natl Acad Sci U S A*. 2005;102(3):673–678.
58. Ho E, Karimi Galougahi K, Liu CC, Bhindi R, Figtree GA. Biological markers of oxidative stress: applications to cardiovascular research and practice. *Redox Biol*. 2013;1:483–491.
59. You BR, Park WH. Suberoyl bishydroxamic acid-induced apoptosis in HeLa cells via ROS-independent, GSH-dependent manner. *Mol Biol Rep*. 2013;40(5):3807–3816.
60. Brechbuhl HM, Kachadourian R, Min E, Chan D, Day BJ. Chrysin enhances doxorubicin-induced cytotoxicity in human lung epithelial cancer cell lines: the role of glutathione. *Toxicol Appl Pharmacol*. 2012;258(1):1–9.
61. Fath MA, Ahmad IM, Smith CJ, Spence J, Spitz DR. Enhancement of carboplatin-mediated lung cancer cell killing by simultaneous disruption of glutathione and thioredoxin metabolism. *Clin Cancer Res*. 2011;17(19):6206–6217.
62. Schnelldorfer T, Gansauge S, Gansauge F, Schlosser S, Beger HG, Nussler AK. Glutathione depletion causes cell growth inhibition and enhanced apoptosis in pancreatic cancer cells. *Cancer*. 2000;89(7):1440–1447.
63. Miriyala S, Spasojevic I, Tovmasyan A, et al. Manganese superoxide dismutase, MnSOD and its mimics. *Biochim Biophys Acta*. 2012;1822(5):794–814.
64. Sena LA, Chandel NS. Physiological roles of mitochondrial reactive oxygen species. *Mol Cell*. 2012;48(2):158–167.
65. Peart MJ, Tainton KM, Ruefli AA, et al. Novel mechanisms of apoptosis induced by histone deacetylase inhibitors. *Cancer Res*. 2003;63(15):4460–4471.
66. Jiang SJ, Dowdy SC, Meng XW, et al. Histone deacetylase inhibitors induce apoptosis in both type I and type II endometrial cancer cells. *Gynecol Oncol*. 2007;105(2):493–500.
67. Sun BB, Fu LN, Wang YQ, et al. Silencing of JMJD2B induces cell apoptosis via mitochondria-mediated and death receptor-mediated pathway activation in colorectal cancer. *J Dig Dis*. 2014;15(9):491–500.
68. Zhou WQ, Feng XY, Han H, Guo SC, Wang GD. Synergistic effects of combined treatment with histone deacetylase inhibitor suberoylanilide hydroxamic acid and TRAIL on human breast cancer cells. *Sci Rep*. 2016;6:28004.
69. Okada K, Hakata S, Terashima J, Gamou T, Habano W, Ozawa S. Combination of the histone deacetylase inhibitor depsipeptide and 5-fluorouracil upregulates major histocompatibility complex class II and p21 genes and activates caspase-3/7 in human colon cancer HCT-116 cells. *Oncol Rep*. 2016;36(4):1875–1885.
70. Wolf BB, Green DR. Suicidal tendencies: apoptotic cell death by caspase family proteinases. *J Biol Chem*. 1999;274(29):20049–20052.
71. Wolf BB, Schuler M, Echeverri F, Green DR. Caspase-3 is the primary activator of apoptotic DNA fragmentation via DNA fragmentation factor-45/inhibitor of caspase-activated DNase inactivation. *J Biol Chem*. 1999;274(43):30651–30656.
72. Lee E, Furukubo T, Miyabe T, Yamauchi A, Kariya K. Involvement of histone hyperacetylation in triggering DNA fragmentation of rat thymocytes undergoing apoptosis. *FEBS Lett*. 1996;395(2–3):183–187.
73. Bolden JE, Peart MJ, Johnstone RW. Anticancer activities of histone deacetylase inhibitors. *Nat Rev Drug Discov*. 2006;5(9):769–784.
74. Glozak MA, Sengupta N, Zhang XH, Seto E. Acetylation and deacetylation of non-histone proteins. *Gene*. 2005;363:15–23.
75. Marks PA, Dokmanovic M. Histone deacetylase inhibitors: discovery and development as anticancer agents. *Expert Opin Investig Drugs*. 2005;14(12):1497–1511.
76. Minucci S, Pelicci PG. Histone deacetylase inhibitors and the promise of epigenetic (and more) treatments for cancer. *Nat Rev Cancer*. 2006;6(1):38–51.
77. Zhao Y, Tan J, Zhuang L, Jiang X, Liu ET, Yu Q. Inhibitors of histone deacetylases target the Rb-E2F1 pathway for apoptosis induction through activation of proapoptotic protein Bim. *Proc Natl Acad Sci U S A*. 2005;102(44):16090–16095.
78. Zhang XD, Gillespie SK, Borrow JM, Hersey P. The histone deacetylase inhibitor suberic bishydroxamate regulates the expression of multiple apoptotic mediators and induces mitochondria-dependent apoptosis of melanoma cells. *Mol Cancer Ther*. 2004;3(4):425–435.
79. Xu W, Ngo L, Perez G, Dokmanovic M, Marks PA. Intrinsic apoptotic and thioredoxin pathways in human prostate cancer cell response to histone deacetylase inhibitor. *Proc Natl Acad Sci U S A*. 2006;103(42):15540–15545.
80. Rosato RR, Maggio SC, Almenara JA, et al. The histone deacetylase inhibitor LAQ824 induces human leukemia cell death through a process involving XIAP down-regulation, oxidative injury, and the acid sphingomyelinase-dependent generation of ceramide. *Mol Pharmacol*. 2006;69(1):216–225.
81. Jiang XJ, Wang XD. Cytochrome C-mediated apoptosis. *Annu Rev Biochem*. 2004;73:87–106.
82. Yang XM, Shi ZL, Zhang N, et al. Suberoyl bis-hydroxamic acid enhances cytotoxicity induced by proteasome inhibitors in breast cancer cells. *Cancer Cell Int*. 2014;14:107.
83. Han MH, Park C, Kwon TK, et al. The histone deacetylase inhibitor trichostatin A sensitizes human renal carcinoma cells to TRAIL-induced apoptosis through down-regulation of c-FLIPL. *Biomol Ther (Seoul)*. 2015;23(1):31–38.

### International Journal of Nanomedicine

Dovepress

## Publish your work in this journal

The International Journal of Nanomedicine is an international, peer-reviewed journal focusing on the application of nanotechnology in diagnostics, therapeutics, and drug delivery systems throughout the biomedical field. This journal is indexed on PubMed Central, MedLine, CAS, SciSearch®, Current Contents®/Clinical Medicine,

Journal Citation Reports/Science Edition, EMBase, Scopus and the Elsevier Bibliographic databases. The manuscript management system is completely online and includes a very quick and fair peer-review system, which is all easy to use. Visit <http://www.dovepress.com/testimonials.php> to read real quotes from published authors.

Submit your manuscript here: <http://www.dovepress.com/international-journal-of-nanomedicine-journal>